

Design and Simulation of Solid State Power Electronic Transformer

D.Srinivasa Rao¹ | Dr. Anupama A. Deshpande¹

¹Department of Electrical Engineering, Shri JITU University, Jhunjhunu, Rajasthan, INDIA

To Cite this Article

D.Srinivasa Rao and Dr. Anupama A. Deshpande¹, "Design and Simulation of Solid State Power Electronic Transformer", *International Journal for Modern Trends in Science and Technology*, 6(8S): 211-217, 2020.

Article Info

Received on 16-July-2020, Revised on 15-August-2020, Accepted on 25-August-2020, Published on 30-August-2020.

ABSTRACT

Recent years has seen rapid development of smart grid and the advancement of renewable resource utilization and technology, solid state power electronic transformers are become an important energy conversion device in modern power systems. In order to provide the functions of electrical transformation, electrical isolation of and integration of both AC and DC ports, three-phase AC to three-phase AC solid state power electronic transformer (SSPET) is proposed. The proposed SSPET has a three stage conversion system. A three-phase PWM rectifier, a HFL DAB DC-DC converter, and a three-phase inverter are major building blocks of the proposed SSPET. By using the simulation platform based on MATLAB/SIMULINK to simulate and verify the proposed three-stage solid state power electronic transformer is realized. The simulation results show that the SSPET realizes the operation of unity power factor on the grid side, output voltage control, electrical isolation, fault isolation, reactive power compensation, power flow control and connection to the DC port.

KEYWORDS: SSPET, three-phase PWM rectifier, HFL, DAB, DC-DC converter, three-phase inverter

I. INTRODUCTION

The power transformer is important equipment in the power system in the traditional industrial and domestic distribution network. Its main function is to provide energy transmission and electrical isolation. Its main advantages are high reliability, better efficiency and low price. But with the development of smart grids, active distribution networks, miniaturization of energy conversion devices and other emerging technologies, the traditional transformers are replacing by solid state power electronic transformers[1]-[3]. The requirements for the intelligent level of distribution equipment are increasing day by day. The shortcomings of the traditional transformer are the lack of continuous regulation, comprehensive control of voltage and currents, its large size, prone to harmonics and environmental pollution due to insulation oil[4]-[5].

Solid state power electronic transformer is also known as intelligent transformer, electronic power transformer or solid-state transformer. Due to its advantages, such as small size and mass, stable output voltage, and good controllability, if SSPET is applied to the power systems; many problems facing by the power system will be solved[6]-[7]. Because the SSPET has the functions of voltage transformation, electrical isolation, and energy transmission, as well as high flexibility and controllability, SSPET has important research significance and good application prospects in the field of AC/DC hybrid distribution networks, promotion of power quality of distribution network and grid connection of distributed power generation sources like PV. Comparing with the traditional transformers, SSPET not only has the

advantages of small volume and mass, but also has high flexibility and controllability. Therefore, improving the flexibility and controllability of SSPET is a key point in research [8]-[10]. The topological structure of SSPET is shown in Fig.1, and it is an AC/DC/AC three-stage structure. This topology uses a high-frequency transformer to achieve voltage level conversion and thus greatly reducing the size and volume of the transformer. Its advantages also include ensuring the controllability of the system and the bidirectional power flow.

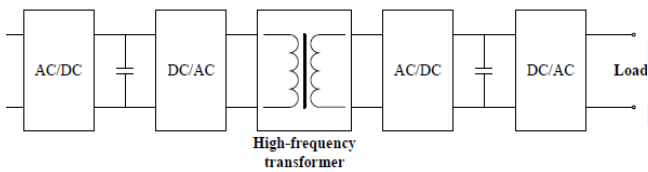


Fig.1. Topology of solid state PET (SSPET)

The SSPET with AC/DC/AC three-stage structure includes input stage, intermediate isolation stage and output stage [11]. Compared with the other structures, it has more conversion structures. It has the best controllable performance and can also realize the functions of power factor correction and reactive power compensation. The three-stage topology is currently the most used topology, which can use lower voltage electronic devices with high voltage input, and its output has good harmonic characteristics [12]. But, due to the direct coupling between the stages, the voltage of each DC bus is not balanced. There may be a large circulating current between the modules, which may damage the power electronic devices due to voltage mismatch across HF link transformer [13]-[14]. Based on the typical three-stage PET topology, this paper proposes a three-stage conversion structure SSPET composed of a three phase PWM rectifier, a HFL DAB DC-DC converter and a three phase inverter [15]. In addition to the advantages of the three-stage SSPET mentioned above, this method can also control the level and phase of the AC side current to largely reduce the influence of the power grid, and achieve the stability in the output voltage at all levels through closed-loop control, with strong controllability and flexibility. Section II provides detailed analysis of three phase PWM rectifier. Section III gives in-depth analysis of HF link DAB based Dc-Dc converter and control methods. Section IV deals with the analysis of three phase inverter section and finally Section V provides MATLAB/SIMULINK results to support the theoretical analysis and design.

II. THREE-PHASE PWM RECTIFIER

A. Three Phase PWM Rectifier Topology

The main circuit topology of the three phase PWM rectifier is shown in Fig.2. In Fig.2 U_A, U_B, U_C are the phase voltages of the three-phase input AC power supply, U_{AB} is the line voltage of A and B supply phases, U_s is the PWM rectifier input line voltage, and U_d is the output DC voltage of the PWM rectifier.

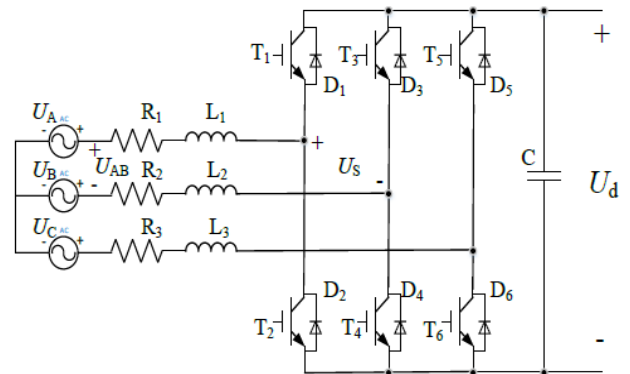


Fig.2. Power circuit of PWM rectifier

Figure 3 shows the gating signals of IGBT switches and are of 50% duty cycle. Each switch conducts for a period of 180° duration. T_2, T_4, T_6 are complimentary switches of T_1, T_3, T_5 respectively and are 180° apart. D is the conduction period of each group of three switches that is for a period of 60° . The six sets of switches are (5,6,1), (6,1,2), (1,2,3), (2,3,4), (3,4,5), (4,5,6).

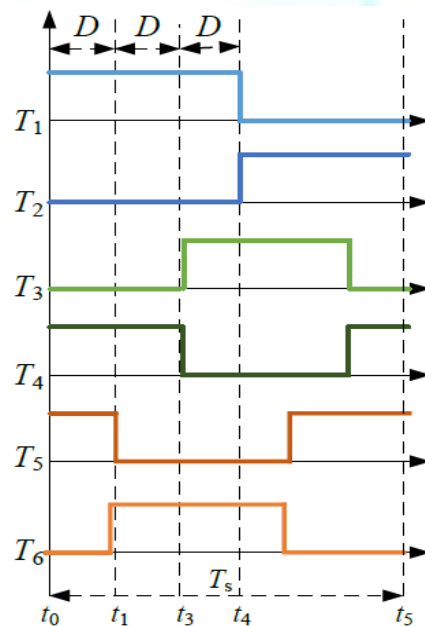


Fig.3 Gating signals of IGBT switches

B. Operating Principle

The equivalent circuit for conduction of a line voltage U_{AB} to input of the rectifier line voltage U_S and U_S to output voltage U_d is shown in Fig.4. The part from U_S to the output voltage U_d is a rectifier circuit, which converts the AC voltage U_S into DC voltage U_d through the H-bridge, and then filters out higher harmonics through the filter capacitor C. In Fig.4, Z_{AB} is the total impedance of all resistors and inductors between U_{AB} and U_S . Therefore, the circuit has the following vector equation

$$U_{AB} = U_S + I_{AB} Z_{AB}, \text{ Where } Z_{AB} = R_1 + R_2 + j\omega L_1 + j\omega L_2, \\ R_1 = R_2 \text{ and } L_1 = L_2 \quad (1)$$

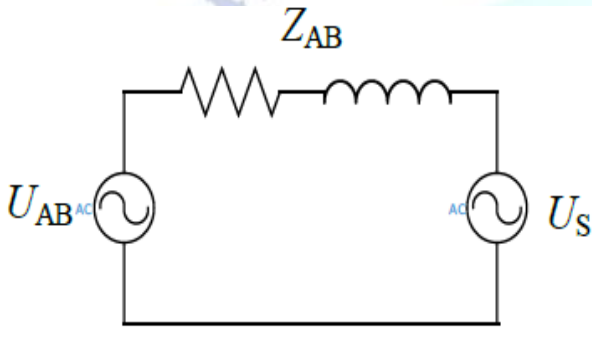


Fig.4 Equivalent circuit of PWM rectifier

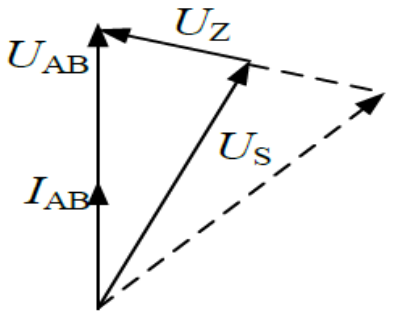


Fig.5 Vector diagram of the equivalent circuit

Fig.5 shows the vector diagram of equivalent circuit shown in Fig.4. In Fig.5 I_{AB} is the line current between U_{AB} and U_S , Z_{AB} is the line impedance. It can be seen from the figure that when the AC side input line voltage U_{AB} remains unchanged, the amplitude and phase of I_{AB} are completely determined by the amplitude and phase of U_S . Therefore, the amplitude and phase of the U_S can be controlled to make the phase of I_{AB} and U_{AB} the same to improve the quality of power supply. Three-phase bidirectional PWM rectifiers can have higher output power compared with unidirectional PWM rectifiers. For a three phase PWM rectifier, when the AC voltage and AC current on the input side are both symmetrical three phase sinusoidal AC.

$$u_{AB}(t) = \sqrt{2} U_{AB} \sin(\omega t) \\ i_{AB}(t) = \sqrt{2} I_{AB} \sin(\omega t) \\ u_{BC}(t) = \sqrt{2} U_{BC} \sin\left(\omega t + \frac{2\pi}{3}\right) \\ i_{BC}(t) = \sqrt{2} I_{BC} \sin\left(\omega t + \frac{2\pi}{3}\right) \\ u_{CA}(t) = \sqrt{2} U_{CA} \sin\left(\omega t - \frac{2\pi}{3}\right) \\ i_{CA}(t) = \sqrt{2} I_{CA} \sin\left(\omega t - \frac{2\pi}{3}\right) \\ U_{AB} = U_{BC} = U_{CA} = U_N, I_{AB} = I_{BC} = I_{CA} = I_N \text{ because of symmetrical voltage and currents.} \quad (2)$$

According to the law of conservation power, the output power on the DC side is equal to the input power on the AC side

$$u_d i_d = u_{AB} i_{AB} + u_{BC} i_{BC} + u_{CA} i_{CA} \quad (3)$$

$$i_d = \frac{u_{AB} i_{AB} + u_{BC} i_{BC} + u_{CA} i_{CA}}{u_d} = \frac{3U_N I_N}{u_d} \quad (4)$$

It is seen that the output current i_d of the three-phase PWM rectifier has only a DC component. For single-phase PWM rectifiers, the output current i_d still has double grid frequency pulsation. Therefore, it is necessary to add a second harmonic filter composed of inductors and capacitors, which will increase the mass and volume of the rectifier. In this three-phase PWM rectifier i_d has six times grid frequency ripple so that the capacitor filter at the output can easily filtered out.

C. Simulation Constructions of Each Leg

Each leg of three-phase PWM rectifier contains two IGBT switches whose switching signals are 180° out of phase. The indirect current control method is used to simulate control signals in each leg of phases A, B and C. Here we take phase A as an example to analyze. The schematic diagram of A-phase indirect current control is shown in Fig.6. When the running time is less than 0.1s, the control circuit is not activated because the circuit output is unstable. When the running time is greater than 0.1s, the control circuit starts to work. The feedback I_N is subtracted from the target current I_{N0} to obtain the error value, and then the A-phase output current is obtained through the PI controller. According to the control scheme, the final phase voltage and phase current phase are the same, so the current multiplied by the resistance and then multiplied by $\sin(\omega t)$ plus the current multiplied by reactance and multiplied by $\sin(\omega t)$ is the voltage drop between U_{AB} and U_S . Subtract it to get U_S .

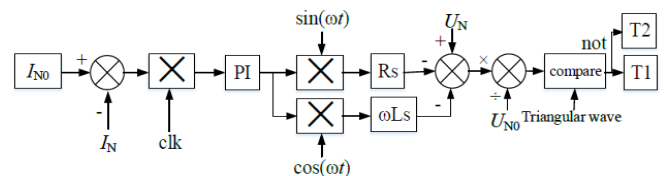


Fig.6 Indirect current control for generation of A-phase switches

The indirect control system controls the output voltage U_D according to the calculated U_S to control the switching circuits of T_1 and T_2 . Since i_d only has a DC component and is proportional to U_D from equation (4), and U_N is constant, so I_N is proportional to the square of U_D , so the control system can achieve the purpose of controlling I_N by controlling U_D . The current control signals for the other two-phases only needs to shift the modulation wave by 120° . Phase B signals are generated by shifting A-phase signals by 120° and phase C signals are generated by further shifting the B-phase signals by another 120° . From Fig.6 T_2 signal is complimentary of T_1 .

III. HF LINK DAB DC-DC CONVERTER

A. Topology of HF Link DC-Dc Converter

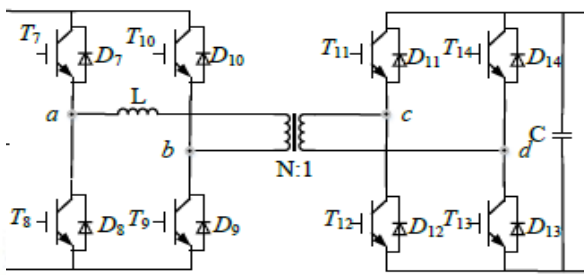


Fig.7 HF link DAB DC-DC converter

The topology of high frequency link DAB based Dc-Dc converter is shown in Fig.7 where V_1 and V_2 are the input and output voltages of the DAB converter. Two H-bridges are linked by a high frequency transformer. U_{ab} , U_{cd} are the input and output voltages of the HF transformer.

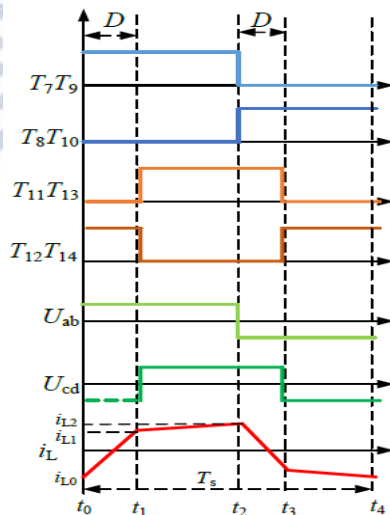


Fig.8 Switching signals of DAB and waveforms

From Fig.8 it is seen that both waves are phase shifted by D . From Fig.8 T_7-T_{14} are the control signals corresponding to the switches, which are all square waves with the same frequency with a duty cycle of 50%. When the switch is turned on, the

control signal output waveform is positive, and when the switch is turned off, the control signal output waveform is zero. D represents the phase difference of the control signal between the switch pairs T_7, T_9 and T_{11}, T_{13} , and T_S is the period of the control signal. U_{ab} and U_{cd} respectively represents the voltage waveform between a, b and c, d. i_L is the waveform of current flowing through the inductor L . i_{L0} , i_{L1} , and i_{L2} represent the current flowing through the inductor at t_0 , t_1 , and t_2 respectively. The direction of phase shift D is the direction of power transmission.

B. Operating Principle of DAB Dc-Dc Converter

The operation of the main circuit of HF DAB DC-DC converter is divided into three parts for detailed analysis: an inverter circuit from V_1 to U_{ab} , a high frequency transformer circuit from U_{ab} to U_{cd} , and a rectifier circuit from U_{cd} to V_2 . In order to keep the output voltage of the DAB circuit remains constant when the input power changes, the DAB circuit uses a single-phase shift control method to control the circuit. The operating principle of the single phase shift control method is as shown below.

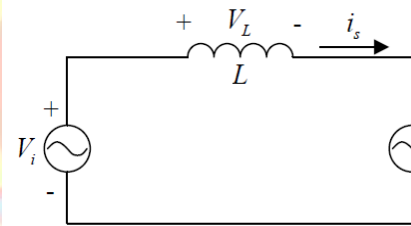


Fig.9 Equivalent circuit of HF transformer

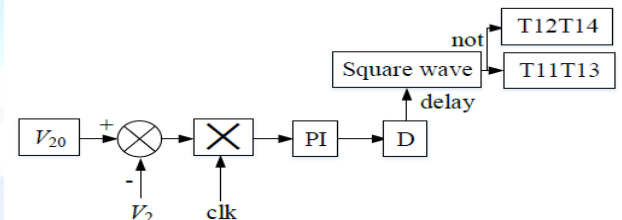


Fig.10 Single phase shift control method

During the period t_0-t_1 , according to the property of the inductance:

$$L \frac{di_L}{dt} = U_{ab} - U_{cd} \quad (5)$$

Where $V_i = U_{ab}$, $V_s = U_{cd}$ and $i_s = i_L$. Since $i_L = i_{L0}$ at t_0 , $U_{ab} = V_1$ and $U_{cd} = -NV_2$ in the t_0-t_1 time period, the inductor current equation is

$$i_L(t) = i_{L0} + \frac{(V_1 + NV_2)}{L}(t_0 - t_1) \quad (6)$$

In the time period t_1-t_2 , Since $i_L = i_{L1}$ at t_1 , $U_{ab} = V_1$, $U_{cd} = NV_2$ at time t_1-t_2 , the inductor current equation is

$$i_L(t) = i_{L1} + \frac{(V_1 - NV_2)}{L}(t_1 - t_2) \quad (7)$$

Due to the symmetry that the output power in the $t_2 - t_4$ period is equal to the output power in the $t_0 - t_2$ period. Let $i_{L0} = -i_{L2}$, therefore, the power transmitted by the circuit is

$$P = \frac{2}{T_S} \int_{t_0}^{t_2} U_{ab}(t) i_L(t) dt = \frac{2NV_1V_2D(\frac{T_S}{2}-D)}{T_S L} \quad (8)$$

If the current i_L has a DC bias of I , $i_{L1} = i_{L0} + I$, $i_{L2} = -i_{L0} + I$, because U_{ab} is exactly half of V_1 in one cycle, so the integral of voltage and bias current is 0 for bias current I . The power due to this part is also zero over a cycle. According to the equation (8), the output voltage V_2 can be kept constant by varying the magnitude of D even the power transmitted by the circuit changes.

C. Simulation of Single Phase Shift Control

The control circuit of HF link DAB DC-DC converter includes two parts: a clock control circuit and a single phase shift control circuit. DAB DC-DC converter and the three-phase PWM rectifier share the same clock control circuit. The phase difference D of the control signal between T_7, T_9 and T_{11}, T_{13} is limited to the range of $(0, T_S/2)$. The output voltage V_2 increases with the increase of D under the same input conditions when D is in the given range. Therefore, the output voltage V_2 can be controlled by controlling D .

IV. THREE PHASE INVERTER

A. Topology of Three Phase Inverter

The topology of three phase inverter is shown in Fig.11. In Fig.11: U_d is the DC side input voltage, N' is the imaginary midpoint or it can be used as virtual neutral point also, $L_4 - L_6$ are the filter inductances, and $R_4 - R_6$ are the load resistances. The output waveforms are shown in Fig.12. From Fig.12: $U_{UN'}$, $U_{VN'}$, $U_{WN'}$ are the voltages of the three points U, V, W relative to the imaginary midpoint N' , U_{UN} is the voltage of the phase A line, $U_{NN'}$ is the neutral point N relative to the imaginary midpoint N' Voltage, U_{AN} is the phase A voltage. The three phase inverter operates in 180° conduction mode in this paper. In this mode each IGBT switch conducts for a period of 180° and the phase voltage is stepped one and continuous, where line voltage waveform is a quasi square wave.

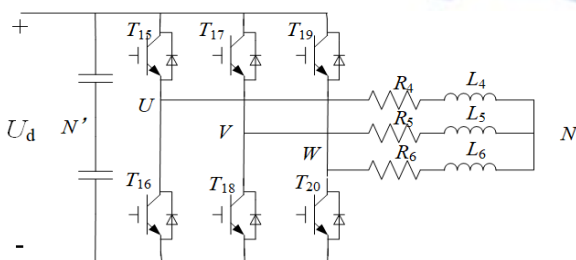


Fig.11 Circuit of three phase inverter

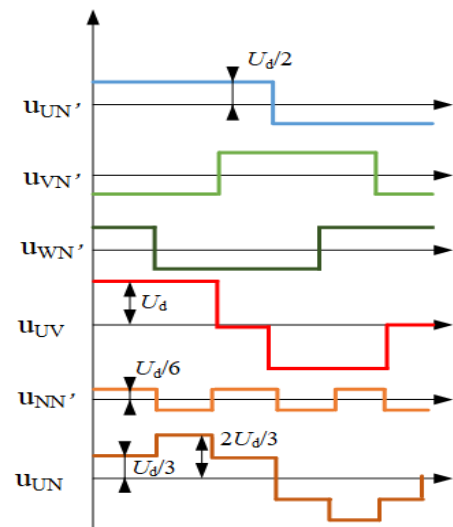


Fig.12 Waveforms of three phase inverter

B. Principle of Operation of Three Phase Inverter

The line voltage U_{UV}, U_{VW}, U_{WU} of each load line can be calculated by equation (9).

$$\begin{aligned} U_{UV} &= U_{UN'} - U_{VN'} \\ U_{VW} &= U_{VN'} - U_{WN'} \\ U_{WU} &= U_{WN'} - U_{UN'} \end{aligned} \quad (9)$$

The phase voltage U_{UN}, U_{VN}, U_{WN} of each phase load can be calculated by equation (10).

$$\begin{aligned} U_{UN} &= U_{UN'} - U_{NN'} \\ U_{VN} &= U_{VN'} - U_{NN'} \\ U_{WN} &= U_{WN'} - U_{NN'} \end{aligned} \quad (10)$$

From equations (9) and (10), the voltage $U_{NN'}$ of the neutral point N relative to the imaginary midpoint N' can be resolved.

$$U_{NN'} = \frac{1}{3}(U_{UN'} + U_{VN'} + U_{WN'}) - \frac{1}{3}(U_{UN} + U_{VN} + U_{WN}) \quad (11)$$

Assume that the load be a three-phase symmetrical load, then $U_{UN} + U_{VN} + U_{WN} = 0$, formula (11) can be converted into:

$$U_{NN'} = \frac{1}{3}(U_{UN'} + U_{VN'} + U_{WN'}) \quad (12)$$

Therefore, $U_{NN'}$ is a rectangular wave with amplitude of $\pm U_d/6$. Also $U_{UN} = U_{UN'} - U_{NN'}$, so the waveform of U_{UN} is the waveform shown in Fig.12.

C. Construction of Simulation Model

The control circuit of the three-phase inverter includes two parts: a clock control circuit and a phase voltage amplitude control circuit. The three-phase inverter and the three-phase PWM rectifier share the same clock control circuit. The phase voltage amplitude control circuit of the three phase inverter is shown in Fig.13.

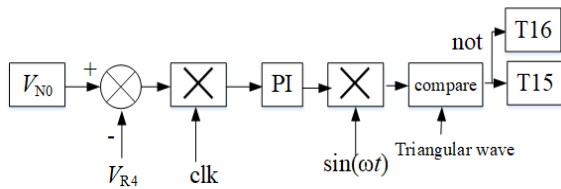


Fig.13 Phase voltage amplitude control block

The voltage U_{R4} output on the load resistance is fed back and subtracted from the target output voltage U_{NO} , and then passes through the PI controller. The output voltage calculated by the PI controller is controlled by the switching signals of T_{15} and T_{16} to achieve the purpose of controlling the output voltage on the load. The output waveform obtained by sinusoidal pulse width modulation has a modulation wave with a frequency of 50 Hz and a carrier wave with a frequency of 10 kHz. Therefore, a filter inductor $L4$ needs to be connected in parallel after the load R_4 to achieve the purpose of filtering high frequency carrier components. The other two-phase voltage control only needs to shift the modulation wave by 120° . The control signals of the complementary IGBT switches must be delayed by twice of the turn-off period of the switches otherwise there may be a chance of Dc supply short circuit.

V. MATLAB SIMULATION ANALYSIS

In this paper, a simulation platform based on MATLAB-SIMULINK, the main circuit and control circuit for Fig.6, Fig.10 and Fig.13 are constructed for the solid state power electronic transformer and are tested, and the simulations are analyzed. Table I provides the assumed system parameters for simulations.

Table I

| Parameter | Value |
|---|-------------|
| Grid side phase voltage U_A, U_B, U_C | 500V |
| Grid side inductance $L_1 - L_3$ | 2mH |
| Grid side resistance $R_1 - R_3$ | 0.2Ω |
| DC side capacitor C | 5mF |
| DC side voltage U_d | 1000V |
| Arm Inductance L | 0.3mH |
| Transformer ratio n | 1 |
| Switching frequency f | 20kHz |
| DC side output voltage V_2 | 1000V |
| filter inductance $L_4 - L_6$ | 2mH |
| Set value of phase voltage | 300V |
| Transmission power P | 100kW |

Fig.14 is three phase supply waveform diagram of grid-side voltage and current obtained through simulation analysis. It can be seen from the figure that through indirect current control, when the circuit reaches a steady state, the phases of the phase A voltage U_A and the current I_A remain the same, the main circuit keeps running at unity power factor, and the circuit has good harmonic

characteristics. The output voltage of output H-bridge remains unchanged at the voltage of 1000V. The output voltage of the main circuit of the rectifier has a short correction time and the output voltage is stable at 1000V.

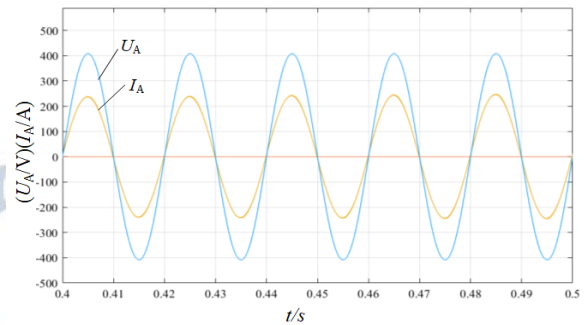


Fig.14 Supply voltage and current waveforms

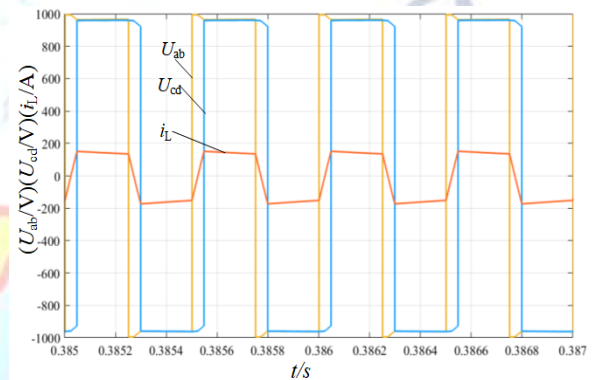


Fig.15 Transformer input and output voltages

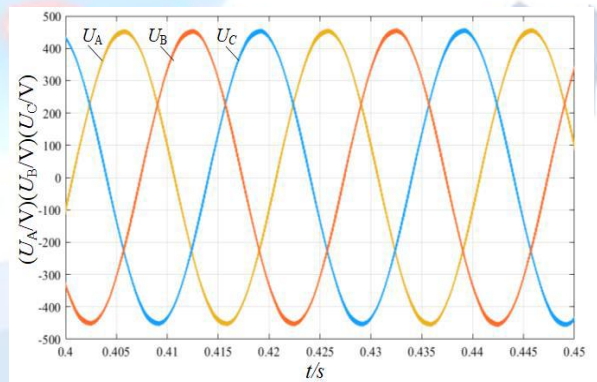


Fig.16 Output waveforms three phase inverter

Figure15 shows the waveform diagram of the voltage on both sides of the isolated HF DAB DC-DC converter and the current flowing through the inductor L obtained through simulation. It is found that U_{ab} and U_{cd} is phase shifted. i_L is the inductor current. Comparing the voltage U_{ab} and U_{cd} obtained by the simulation when the circuit reaches the steady state, the amplitudes are almost same. The waveform of the current i_L and the waveform obtained from the theoretical analysis above show that the simulation analysis is consistent with the theory and the simulation results are as expected. Fig.16 shows the output voltage waveform diagram of the three phase

inverter obtained through simulation. It is observed from the figure that the output voltage is a balanced three-phase sinusoidal voltage, with better harmonic characteristics, and the amplitude of the output voltage is constant.

VI. CONCLUSION AND FUTURE SCOPE

This paper proposes a three-stage solid state power electronic transformer. The operation principle and control method of three-phase PWM rectifier, HF DAB DC-DC converter, and three-phase inverter are analyzed in detail. Finally, a simulation platform setup based on MATLAB-SIMULINK was realized to verify the solid state power electronic transformer. The solid state power electronic transformer can realize grid-side unit power factor operation, ensuring that the grid-side voltage and current are in the same phase, so as to realize the control both active and reactive powers. The output voltage of the solid state power electronic transformer is controllable, and it can keep the output voltages are at constant magnitude and balanced. The solid state power electronic transformer has both an AC port and a DC port, which can be connected to a traditional AC system or a renewable energy sources. This method can also be used to integrate renewable sources like PV, wind in to the AC grid.

ACKNOWLEDGMENT

I would like to express my deep gratitude to my co guide Dr. K. Chiranjeevi, Associate professor, department of Electrical Engineering for his valuable and constructive suggestions towards the completion of this research paper. I would like to acknowledge Battula Greeshma, Scientist-C, ISTRAC, ISRO, for her constructive timely suggestions valuable technical inputs. Not but not least, I am indebted to Prof. B. Subba Reddy towards his valuable contributions in completing this paper.

References

- [1] Bifaretti S, Zanchetta P, Watson A, et al. Advanced power electronic conversion and control system for universal and flexible power Management [J]. IEEE Transactions on Smart Grid, 2011(2) : 231- 243.
- [2] Hugo N, Stefanutti P, Pellerin M, et al. Power electronics traction transformer[C]//Proceedings of 2007 European Conference on Power Electronics and Applications, Aalborg, Denmark : IEEE 2007 : 1- 10.
- [3] Y. Huang, C. Mao, J. Lu and S. Fan, "Study on control strategy for power electronic transformer in power system," Relay., vol.32, no.6, pp.35-39, Mar.2004.
- [4] J. Zhao, "Simulation study of a power electronics transformer with constant output voltage," Automation of Electric Power Systems., vol.27, no.18, pp.30-33, Sept.2003.
- [5] Z. Lu, G. Zhao, D. Yang and X. Zeng, "Overview of research on power electronic transformer in distribution network," Proceedings of the CSUEPSA., vol.28, no.5, pp.48-50, May.2016.
- [6] J. Han, Y. Li, Y. Cao and et al, "A new DC microgrid architecture based on MMC-SST and its control strategy," Power System Technology., vol.40, no.3, pp.733-740, Mar.2016.
- [7] S. Hu and H. Zou, " The topology structure of a cascaded power electronic transformer," Journal of Shanghai Dianji University., vol.21, no.3, pp.36- 47, 2018.
- [8] Q. Chen, Y. Ji, Y. Pan and J. Wang. "Review of power electronic transformer topologies applied to distribution system," Advanced Technology of Electrical Engineering and Energy., vol.34, no.3, pp.41-48, Mar.2015.
- [9] Wang Xinyu , Liu Jinjun , Ouyang Shaodi et al . Research on unbalanced-load correction capability of two SST topologies[J] . IEEE Transactions on Power Electronics, 2015, 30(6) : 3044-3056.
- [10] Briz F, Lopez M, Rodriguez A, et al. Modular SSTs : modular multilevel converter versus cascaded h-bridge solutions[J] . IEEE Industrial Electronics Magazine, 2016 , 10(4) : 6-19.
- [11] Ahmed H F, Cha H, Khan A A, et al. A highly reliable single-phase high-frequency isolated double step-down AC-AC converter with both noninverting and inverting operations[J] . IEEE Transactions on Industry Applications, 2016, 52(6) : 4878-4887.
- [12] Zhao Chuanhong, Dujic D, Mester A, et al. Power electronic traction transformer—medium voltage prototype[J] . IEEE Transactions on Industrial Electronics , 2014, 61(7) : 3257-3268.
- [13] Besselmann T , Mester A , Dujic D . Power electronic traction transformer : efficiency improvements under light-load conditions[J] . IEEE Transactions on Power Electronics, 2014, 29(8) : 3971-3981.
- [14] C. J. Posada, J. M. Ramirez and R. E. Correa, "Modeling and simulation of a solid state transformer for distribution systems," 2012 IEEE Power and Energy Society General Meeting, San Diego, CA, USA, 2012, pp. 1-6.
- [15] Z. Ni, "Research and Design of Three-Stage Power Electronic Transformer," 2021 11th International Conference on Power, Energy and Electrical Engineering (CPEEE), Shiga, Japan, 2021, pp. 195-201.